Journal of The Electrochemical Society, **146** (2) 744-748 (1999)
S0013-4651(98)05-007-1 CCC: $7.00 © The Electrochemical Society, Inc.

Pattern Planarization Model of Chemical Mechanical Polishing

Dar-Zen Chen[z] and Bor-Shin Lee

Department of Mechanical Engineering, National Taiwan University, Taipei, Taiwan 10660

A polishing model of chemical mechanical polishing (CMP) is established with consideration of the effects of pattern density. This paper focuses on mechanical polishing behaviors and isolates the roles of chemical effects when patterns exist. A three-link manipulator, which is in equilibrium with the polishing motion of CMP, is adopted to study the kinematics of CMP. Time-dependent removal rate formulas are presented by considering the decrement of pattern step height. The necessary parameters, wear coefficient, and loading density coefficient are obtained by fitting to experimental data and the complete model is presented.
© 1999 The Electrochemical Society. S0013-4651(98)05-007-1. All rights reserved.

Manuscript submitted May 4, 1998; revised manuscript received August 28, 1998.

Chemical mechanical polishing (CMP) is one of the most effective planarization technologies for achieving smaller feature size and multilevel interconnections for the integrated circuit (IC) industry.[1-3] CMP is used for planing interlevel dielectrics (ILDs) and metal films in general and can be extended to many planarization techniques in device fabrication.[4,5] Because of its ability to meet the increasingly stringent lithographic requirements of device manufacture on silicon wafer, CMP is receiving increasing attention in the fabrication of ultralarge scale integrated/very large scale integrated (ULSI/VLSI) chips.

The polishing mechanism, process control, and basic understanding of CMP remain essentially on the experiential level. There is a variety of physical and chemical effects that are involved in the CMP process and analysis from various scienctific and engineering fields is needed.[6] It is assumed that the polishing mechanism is a function of both chemical and mechanical effects.[7] Chemical effects are achieved by applying the slurry to the wafer and changing the chemical properties of the wafer. Chemical reactions between slurries and the wafer surface change the solubility and mechanical properties of the wafer surface. The mechanical process is affected by the down force, the rotational speeds of the pad and the wafer, the density and viscosity of the slurry, and the material and the surface microstructures of pad and carrier film. Most previous research on the CMP modeling had focused on planarization behavior in polishing blanket wafers. The Preston equation,[8] an experiential equation for glass polishing, summarized the mechanical removal rate and hence provided a way for process control. Cook[9] reviewed the mechanics and chemical polish for glass polishing and proposed a microcutting mechanism to simulate the breaking of chemical bonds. Runnels and Eyman[7] analyzed the fluid film between wafer and pad. Based on statistical method and elastic theory, Liu et al.[10] showed that the removal rate is dependent on the elastic modulus of the slurry particle and polished film. Tseng and Wang[11] modified the Preston equation and showed that the removal rate is proportional to the terms $P^{5/6}$ and $V^{1/2}$. Wang et al.[12] showed that the Von Mises stress correlates with polishing nonuniformity while the normal stress does not and the CMP uniformity can be improved by decreasing polishing pad and carrier film compressibility. Chekina et al.,[13] based on the contact mechanics, developed a wear-contact model of the CMP process which includes parameters such as pad deformation and wafer surface evolution. However, the polishing of the blanket wafer and the patterned wafer is different. The element configuration on the wafer affects the results of CMP planarization and can behave in a different way.

In this paper, a polishing model of CMP that considers the patterns on the wafer is established. The chemical effects are taken as constant in the polishing model since the reactants used are the same. The individual removal rate of upper and lower feature surfaces can be obtained from the assumption that distinct pressures are exerted on different surfaces. In this model, the polishing motion is also studied based on the principle of kinematic inversion. Experimental results conduce to necessary parameters and the verification of the CMP model. This semiexperimental model allows quantitative evaluation of a given CMP process and provides a basis for process optimization to meet specific technological requirements for planarization.

Polishing Model

A schematic diagram of the CMP is shown in Fig. 1. The wafer is mounted upside down on the wafer carrier and rotates above a pad sitting on a table. The slurry that flows between the wafer and the pad dissolves and removes the wafer layer. Figure 2a shows a schematic cross section of wafer surface. There are elements constructed on the wafer surface with different features, and the pad is deflected by the down force. An initial step height, h_0, between the upper and lower feature surfaces is shown in Fig. 2b. The polished thicknesses on upper and lower feature surfaces are denoted as δ_U and δ_L. For the upper feature surface area, A_U, and the lower feature surface area, A_L, we have

$$A = A_U + A_L \qquad [1]$$

where A is the total wafer area.

The pattern density, D, can be defined as

$$D = \frac{A_U}{A} \qquad [2]$$

Note that the variation of the applied pressure and the polishing velocity within the considered region, A, may be neglected. In the

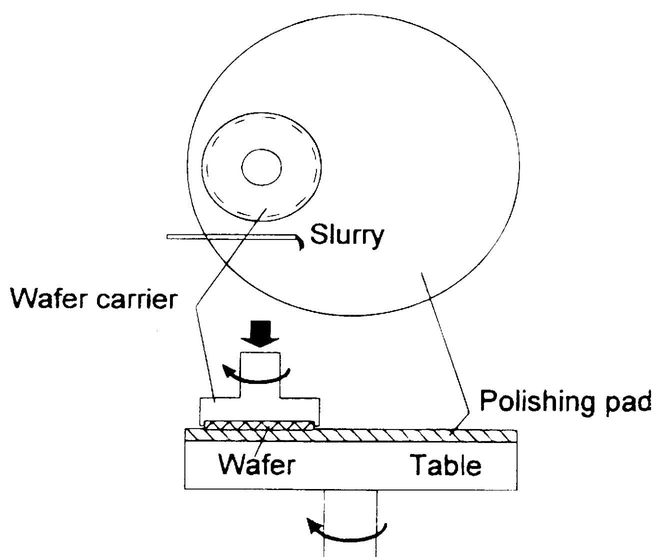

Figure 1. Schematic diagram of CMP polisher.

[z] E-mail: dzchen@ccms.ntu.edu.tw

Journal of The Electrochemical Society, **146** (2) 744-748 (1999)
S0013-4651(98)05-007-1 CCC: $7.00 © The Electrochemical Society, Inc.

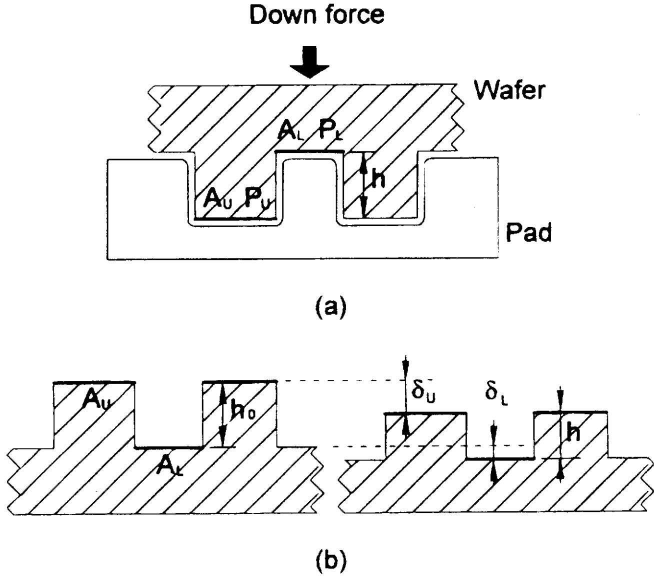

Figure 2. (a) Cross section of the patterns and pad profiles. (b) Patterns before and after polishing.

following, polishing behavior with the existence of patterns is considered with the following assumptions

1. The material removal is anisotropic downward and has no effect on the sidewall of the profiles, i.e.

$$P_U A_U + P_L A_L = PA \quad [3]$$

where P_U and P_L are the pressures on the upper and lower feature surfaces, and P is the total pressure.

2. The pressures on the upper and lower surfaces are directly proportional to the step height, h, i.e.

$$P_U - P_L = \alpha h \quad [4]$$

where the loading density coefficient, α, indicates the stiffness of the polishing pad.

3. The polishing mechanism of every point on the wafer follows the linear wear equation[12]

$$W = \frac{KLS}{H} \quad [5]$$

where W is the wear volume, K is the wear coefficient, L is the down force of the pad onto the wafer, S is the polishing path of the polished point, and H is the hardness of the polished material.

From Eq. 2, 3, and 4, P_U and P_L can be written as

$$P_U = P + \frac{A_L}{A}\alpha h = P + (1 - D)\alpha h \quad [6]$$

and

$$P_L = P - \frac{A_U}{A}\alpha h = P - D\alpha h \quad [7]$$

Since the wear volume is equal to the polished thickness, δ, times the polished area, Eq. 5 can be rewritten as

$$\delta = \frac{K}{H}\frac{L}{A}S \quad [8]$$

By taking the derivative of Eq. 8, the removal rate can be written as

$$\dot{\delta} = \frac{d}{dt}\left(\frac{K}{H}\frac{L}{A}S\right) = \frac{K}{H}PV_p \quad [9]$$

By substituting Eq. 6 and 7 into Eq. 9, the removal rate of the upper and lower surfaces, $\dot{\delta}_U$ an $\dot{\delta}_L$, can be written as

$$\dot{\delta}_U = \frac{K}{H}V_p\left[P + (1 - D)\alpha h\right] \quad [10]$$

and

$$\dot{\delta}_L = \frac{K}{H}V_p(P - D\alpha h) \quad [11]$$

Since the rate of decrease in step height is the difference of the removal rate between the upper and lower surfaces, we have

$$\frac{dh}{dt} = -(\dot{\delta}_U - \dot{\delta}_L) \quad [12]$$

or by substituting Eq. 10 and 11 into Eq. 12, we have

$$\frac{dh}{dt} + \frac{K}{H}V_p\alpha h = 0 \quad [13]$$

Equation 13 can be solved with initial step height h_0 as

$$h = h_0 \exp\left(-\frac{K}{H}V_p\alpha t\right) \quad [14]$$

By substituting Eq. 14 into Eq. 10 and 11, we have

$$\dot{\delta}_U = \frac{K}{H}V_p\left[P + (1 - D)\alpha h_0 \exp\left(-\frac{K}{H}V_p\alpha t\right)\right] \quad [15]$$

and

$$\dot{\delta}_L = \frac{K}{H}V_p\left[P - D\alpha h_0 \exp\left(-\frac{K}{H}V_p\alpha t\right)\right] \quad [16]$$

Equations 15 and 16 show the time-dependant removal rate on the upper and lower feature surfaces of the wafer. The variables in these equations are K, H, P, α, and V_p. The polishing velocity, V_p, can be adjusted by changing the angular velocity of the table and carrier. However, the polishing velocity is a time-dependent term, and it differs from point to point. In the following section, the kinematics of CMP are studied.

Kinematics

Figure 3 shows a two-axis polisher in which points O_t and O_w are the rotational centers of the polishing pad and the wafer, respectively. The distance between points O_t and O_w is a_1, and points O_w and A is a_2. For a referenced point A on the wafer which is coincident with a point B on the pad, the relative velocity of point B to A is defined as the polishing velocity at point A.

It is known that kinematic inversion of a mechanism in no way changes the relative motion between its links no matter which link is held fixed.[13] Accordingly, the geometry of the polisher shown in Fig. 3a can be expressed as a three-link open-loop arm as shown in Fig. 3b. The coordinate systems can be established according to the *D-H* convention.[16] For link i, the $\mathbf{z}_{i-1}$ axis is the rotational axis of link i since link i rotates with respect to link (i − 1) along $\mathbf{z}_{i-1}$. The $\mathbf{x}_i$ axis (perpendicular to $\mathbf{z}_i$) is normal to $\mathbf{z}_{i-1}$ and pointing away from it, and the $\mathbf{y}_i$ axis completes the right-handed coordinate system. To describe the relationship between link i and link (i − 1), the joint angle, $\theta_i = \theta_{i,i-1}$, is defined as the angle from the $\mathbf{x}_{i-1}$ axis to the $\mathbf{x}_i$ axis along the $\mathbf{z}_{i-1}$ axis.

The table rotating with respect to ground is just link 0 with respect to link 1. The joint angle θ_1 is the angle from link 1 to link 0. From the kinematic inversion, the angular velocity of the table, ω_t, can be expressed by the derivation of joint angle $\dot{\theta}_1$ that is the same as ω_t in magnitude but opposite in direction. That is

$$\omega_t = -\dot{\theta}_1 \quad [17]$$

and the angular velocity of wafer, ω_w, can be written as

$$\omega_2 = \dot{\theta}_2 \quad [18]$$

The angular velocity of each link and the linear velocity at the origin ($\mathbf{x}_i$, $\mathbf{y}_i$, $\mathbf{z}_i$) coordinate system can be derived from the forward recursive equations as

$$^{i}\omega_i = {}^{i}\mathbf{R}_{i-1}({}^{i-1}\omega_{i-1} + \dot{\theta}_{i,i-1}{}^{i-1}\mathbf{z}_{i-1}) \quad [19a]$$

and

$$^{i}\mathbf{v}_i = {}^{i}\mathbf{R}_{i-1}{}^{i-1}\mathbf{v}_{i-1} + {}^{i}\boldsymbol{\omega}_i \times {}^{i}\mathbf{p}_i \quad [19b]$$

where $^{i}\mathbf{R}_{i-1}$ is the rotation matrix from the ith to the $(i-1)$th coordinate system, $^{i-1}\mathbf{z}_{i-1}$ is $[0, 0, 1]^T$, and $^{i}\mathbf{p}_i$ is the position vector defined from o_{i-1} to o_i.[17]

For the kinematic model shown in Fig. 4, $^{1}\mathbf{p}_1 = [a_1, 0, 0]^T$, $^{2}\mathbf{p}_2 = [a_2, 0, 0]^T$ and with $^{0}\omega_0 = {}^{0}\mathbf{v}_0 = [0, 0, 0]^T$, we have

$$^{i}\mathbf{R}_{i-1} = \begin{bmatrix} \cos\theta_i & \sin\theta_i & 0 \\ -\sin\theta_i & \cos\theta_i & 0 \\ 0 & 0 & 1 \end{bmatrix} \quad [20]$$

and from Eq. 19a and b, we have

$$^{1}\boldsymbol{\omega}_1 = {}^{1}\mathbf{R}_0({}^{0}\boldsymbol{\omega}_0 + \dot{\theta}_1{}^{0}\mathbf{z}_0) = [0\ 0\ \dot{\theta}_1]^T \quad [21a]$$

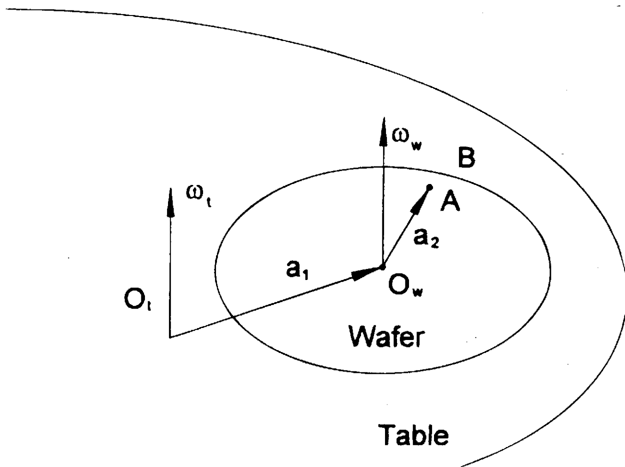

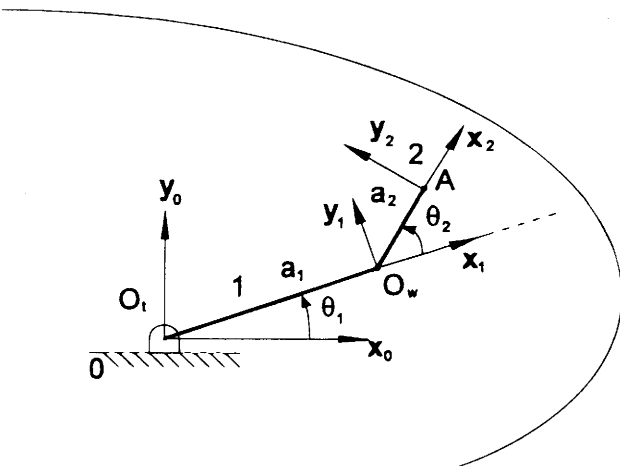

Figure 3. (a) The geometry of CMP polisher. (b) A three-link manipulator model of CMP with D-H conventions.

$$^{2}\boldsymbol{\omega}_2 = {}^{2}\mathbf{R}_1({}^{1}\boldsymbol{\omega}_1 + \dot{\theta}_2{}^{1}\mathbf{z}_1) = [0\ 0\ \dot{\theta}_1 + \dot{\theta}_2]^T \quad [21b]$$

$$^{2}\mathbf{V}_2 = {}^{2}\mathbf{R}_1{}^{1}\mathbf{V}_1 + {}^{2}\boldsymbol{\omega}_2 \times {}^{2}\mathbf{p}_2 = [a_1 \sin\theta_2\dot{\theta}_1\ \ a_1\cos\theta_2\dot{\theta}_1\ \ + a_2(\dot{\theta}_1 + \dot{\theta}_2)\ 0]^T \quad [21c]$$

Let the angular velocity ratio, k_v, be defined as the angular velocity ratio of wafer to pad, i.e,

$$k_v = -\frac{\dot{\theta}_2}{\dot{\theta}_1} \quad [22]$$

By rewriting Eq. 21c, the magnitude of the polishing velocity can be written as

$$|V_p| = |\dot{\theta}_1|(a_1^2 + a_2^2(k_v - 1)^2 - 2a_1a_2(k_v - 1)\cos\theta_2)^{1/2} \quad [23]$$

From Eq. 23, it can be seen that the polishing velocity of a point varies with position. The values of a_1, a_2, and θ_2 indicate the position of a considered point and only the variable θ_2 is a function of time. It can be found that the polishing velocity will repeat for θ_2 passing through an angle 2π. The period of polishing velocity can be as θ_2 goes from 0 to 2π. To obtain the average polishing velocity, the polishing path of a point during a period is needed. The polishing path, S, can be calculated by integrating the polishing velocity in Eq. 23

$$S = \int_0^{2\pi}\left|\frac{1}{k_v}\right|\sqrt{a_1^2 + a_2^2(k_v - 1)^2 - 2a_1a_2(k_v - 1)\cos\theta_2}\,d\theta_2 = 4\left|\frac{G}{k_v}\right|E(m) \quad [24]$$

where

$$E(m) = \int_0^{\pi/2}(1 - m\sin^2\theta)^{1/2}d\theta \quad [25a]$$

$$m = \frac{4a_1a_2(1 - k_v)}{G^2} \quad [25b]$$

and

$$G = a_1 + a_2 - k_va_2 \quad [25c]$$

Equation 25a is the complete elliptic integral, which has been tabulated and is readily available in most mathematical handbooks such as Peiroc.[18] From Eq. 24, the average polishing velocity can be obtained

$$V_{avg} = \frac{S}{2\pi/|\dot{\theta}_2|} = \frac{S}{2\pi/|k_v\dot{\theta}_1|} = \frac{2}{\pi}|\dot{\theta}_1G|E(m) \quad [26]$$

By ignoring the small variations in polishing velocity, the average polishing velocity can be used instead of the polishing velocity. Substituting Eq. 26 into Eq. 15 and 16, we have

$$\dot{\delta}_U = \frac{2K}{\pi H}|\dot{\theta}_1G|\left[P + (1 - D)\alpha h_0h_n\right]E(m) \quad [27]$$

and

$$\dot{\delta}_L = \frac{2K}{\pi H}|\dot{\theta}_1G|\left[P - D\alpha h_0h_n\right]E(m) \quad [28]$$

where h_n is the normalized step height and is defined as the ratio of step height to initial step height, i.e.,

$$h_n = \frac{h}{h_0} = \exp\left(-\frac{2K}{\pi H}|\dot{\theta}_1G|E(m)\alpha t\right) \quad [29]$$

From Eq. 27 and 28, it can be seen that the removal rate of the upper feature surface of the wafer will decay with time while the removal rate of the lower feature surface will increase with time due to the decrease in step height. When the step height is close to zero, the

S0013-4651(98)05-007-1 CCC: $7.00 © The Electrochemical Society, Inc.

removal rate of upper and lower feature surfaces are similar to each other. The normalized step height, h_n, in close proximity to zero indicates a good planarization effect. The initial state of normalized step height is one. Hence, normalized step height, h_n, can be used as a planarization index. To improve the throughput, the normalized step height has to decay faster. This can be achieved by adjusting the polishing parameters in these equations.

In Eq. 29, the K term indicates the chemical effects in CMP. To improve the chemical erosion, K can be increased, improving the polishing effect and making the polishing time shorter. The H term indicates the hardness of the polished material. Polishing a harder material requires a longer planarization time. From Eq. 27 and 28, the pressure affects the removal rate on the upper and lower surfaces but, from Eq. 29, it does not influence the normalized step height. This implies that high pressure can only improve the removal rate and that it will bring about no improvement in planarization. From Eq. 29, the α term indicates the stiffness of the polishing pad. From the equation, it can be seen that a hard pad is better than a soft pad because the planarization speed with a hard pad is faster than that with a soft pad.

Model Parameters

Two experiments are needed to acquire the necessary parameters, K and α, in the polishing model. The first experiment adopts the polishing of a blanket wafer to obtain the wear coefficient K while isolating the influences of the parameter α. In order to investigate the loading density α, the second experiment employs the polishing of a wafer with patterns on its surface for the reason that α only functions when there are step heights.

Parameter K.—The wear coefficient K is associated with material properties, slurry concentration, and chemical processes during CMP. The value of K indicates the chemical erosion at a specific point. Its behavior will vary from point to point because it is both pressure and motion dependent. The down pressure and relative motion will affect the fluxion of slurry, distribution of slurry particles, and chemical erosion. Accordingly, the value of the wear coefficient will alter under individual polishing conditions. It can be assumed that the wear coefficient is a function of down pressure, table speed, and the angular velocity ratio, i.e.

$$K = K_c P^m \dot{\theta}_1{}^n k_v^j \qquad [30]$$

where K_c is the common polishing coefficient that indicates the constant chemical effects with fixed down pressure, the relative motion of pad and wafer, and the same pad conditioning effects.

The experimental data cited below are from Liu.[19] The experimental conditions are (*i*) a 6 in. blanket wafer with thermal silicon dioxide film deposited on its surface; (*ii*) carrier speed: 42 rpm; (*iii*) down pressure: 4-7 psi; (*iv*) table speed: 20-50 rpm; and (*v*) polishing time: 120 s.

Thicknesses before and after polishing are measured at 0.6 cm intervals at twelve points along the radius on a wafer. Then the average removal rate is obtained from the average value of polishing thickness obtained from these twelve points. For a given value of down pressure and table speed, a removal rate is obtained.

The theoretical removal rate can be obtained by averaging the values at these 12 points. That is

$$\frac{1}{12}\sum_{i=1}^{12} \dot{\delta}_i = \frac{KP}{H}\frac{1}{12}\sum_{i=1}^{12} V_{p_i} = \frac{K_c P^m \dot{\theta}_1 k_v^j}{H} P\overline{V} \qquad [31]$$

where $\overline{V}$ is the average polishing velocity at these twelve points.

The average removal rate data are plotted against carrier speed in Fig. 4 for a variety of pressures. By assuming that the theoretical removal rate matches the experimental data, the method of least square fits can be used to obtain the values of K_c, m, n, and j. The data are fitted to the model developed above with constant P. The value of K_c is 24.72, m is 0.30, n is −0.79, and j is −0.14. Figure 5 shows the relation of removal rate and pressure under a given table speed.

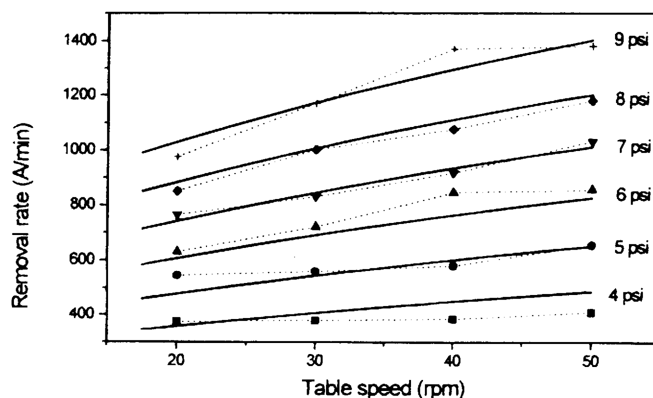

Figure 4. Removal rate vs. table speed for given pressure.[11]

Parameter α.—The loading density coefficient α is associated with the pad material properties. The pad is in compliance either with the upper or lower pattern surfaces. The experimental conditions are (*i*) carrier speed: 42 rpm; (*ii*) table speed: 20 rpm; (*iii*) down pressure: 7 psi; and (*iv*) BPSG covered patterns (the hardness relative to thermal dioxide is about 0.6).

From the polishing conditions above, the wear coefficient K is assumed to be the same with the result above and can be obtained from Eq. 30 as 30.91 and the average polishing velocity of twelve points can be obtained as 0.3824 m/s. From the model developed above, the step height decay obeys Eq. 29. It is assumed that the theoretical step height matches the experimental data cited from the work by Liu.[19] The step height before polishing is the initial step height. The method of least square fits can be used to obtain a value for α of 0.7974 TPa/m. Figure 6 shows the normalized step height decays with time.

Discussion

The complete CMP model is summarized and rewritten as follows

$$\dot{\delta}_U = \frac{2K}{\pi H}\left|\dot{\theta}_1 G\right|(P + (1 - D)\alpha h_0 h_n)E(m) \qquad [32]$$

$$\dot{\delta}_L = \frac{2K}{\pi H}\left|\dot{\theta}_1 G\right|(P - D\alpha h_0 h_n)E(m) \qquad [33]$$

$$h_n = \exp\left(-\frac{2K}{\pi H}\left|\dot{\theta}_1 G\right| E(m)\alpha t\right) \qquad [34]$$

The unknown parameters can be obtained from the above procedure as

$$K = 24.72 \cdot P^{0.3} \cdot \dot{\theta}_1^{-0.79} \cdot k_v^{-0.14} \qquad [35]$$

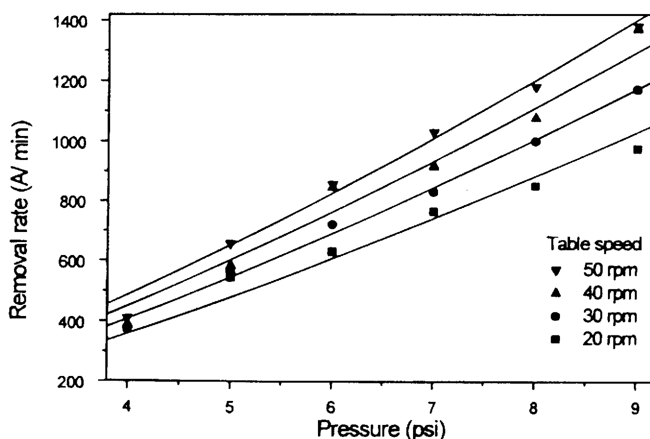

Figure 5. Removal rate vs. pressure for given table speed.[11]

S0013-4651(98)05-007-1 CCC: $7.00 © The Electrochemical Society, Inc.

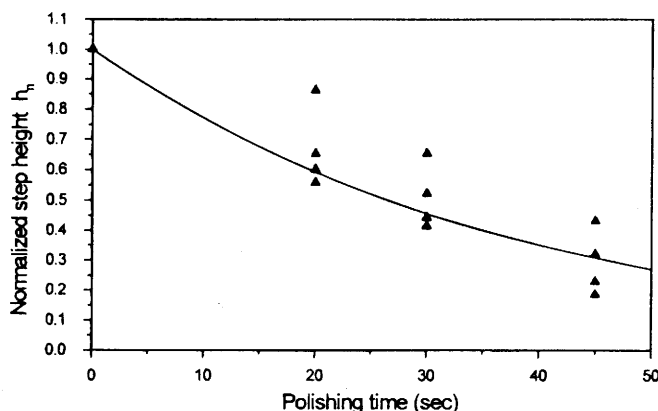

Figure 6. Normalized step height vs. time.

$$\alpha = 0.7974\ TPa/m \quad [36]$$

Equation 35 shows that the applied pressure, table speed, and angular velocity greatly influence the wear coefficient. A higher applied pressure increases the ability of the pad to catch the particles in the slurry and raises the wear coefficient. In addition, higher pressure can also enhance chemical erosion as a consequence of stress-assisted chemical attack by an aggressive slurry.[11] From Eq. 26, it can be seen that by increasing the table speed the polishing velocity increases and the polishing process is enhanced. However, from Eq. 35, a higher table speed decreases the effective corrosion ability and decreases the wear coefficient under the same pad conditioning condition. Hence, increasing the polishing velocity by raising the table speed does not give a proportionate increase in removal rate.

The angular velocity ratio k_v determines the relative motion of a moving table and carrier. The two-dimensional fluid streamline coincides when the angular velocity ratio is maintained. The fluid motion can be related to slurry distribution that makes the chemical erosion change. A theoretical relation for the streamline to slurry distribution and the influences on removal rate is needed to develop for the two-dimensional condition. In Eq. 35, an experimental solution is introduced above to relate the angular velocity ratio to the chemical effects. The experimental result shows that increasing the angular velocity ratio will cause the wear coefficient to decrease. This phenomenon is like the effect produced by increasing the table speed. A higher angular velocity ratio also tends to carry the abrasive particles away in the flowing slurry. Note that, the relation between the wear coefficient and the angular velocity ratio must be recounted for a minus angular velocity ratio.

The experiment on pattern planarization shows how to obtain the loading density α by assuming a constant loading density. However, from Fig. 6, it can be seen that the value of α is influenced by the pattern density and does not behave as a constant. It can be understood that the pad in compliance with the wafer surface will be influenced by the pattern. The line and recess patterns deform the pad in a different curvature when the recess width changes. This makes h_n dependent on the pattern density. In other words, the step height may prevent the lower surface from being in contact with the pad when the flexibility of the pad is not great enough. The polishing task occurs only on the upper feature surface and the lower feature surface only undergoes corrosion. Hence, the step height decay is dependent on the pattern density.

Conclusion

A CMP model that considers the pattern density on a wafer surface is developed. The results indicate that the polishing behaviors on the upper and lower feature surfaces are affected by the patterns. Time-dependent removal rate formulas are presented to describe the influences on the planarization of patterns. From the kinematics, the polishing velocity is a function of the angular velocity of the carrier and table, the distance between the center of the table and the carrier, and the distance of a polished point to the carrier center. The wear coefficient and loading density coefficient are obtained by matching the model with the experimental data. The influences of mechanical motion on the chemical effects during CMP process are also discussed.

The National Taiwan University assisted in meeting the publication costs of this article.

List of Symbols

- D pattern density defined as the area ratio of upper feature to total area
- H hardness of polished film
- h_0 initial step height, Å
- h_n normalized step height
- K_c the common polishing coefficient
- k_v angular velocity ratio defined as the ratio of $\dot{\theta}_2$ to $(-\dot{\theta}_1)$
- P applied pressure, kPa
- V_p polishing velocity, m/s
- α loading density coefficient, N/m^3
- $\dot{\delta}_L$ removal rate on lower surface, Å/min
- $\dot{\delta}_U$ removal rate on upper surface, Å/min

References

1. K. Skidmore, *Semicond. Int.*, 115 (1988).
2. F. Malik and R. Solanki, *Thin Solid Films*, **193**, 1030 (1990).
3. M. A. Martines, *Solid State Technol.*, **26** (1994).
4. J. Warnock, *J. Electrochem. Soc.*, **138**, 2398 (1991).
5. F. B. Kaufman, D. B. Thompson, R. E. Broadie, M. A. Jaso, W. L. Guthrie, D. J. Pearson, and M. B. Small, *J. Electrochem. Soc.*, **138**, 3460 (1991).
6. I. Ali, S. R. Roy, and G. Shinn, *Solid State Technol.*, 63 (1994).
7. S. R. Runnels and L. M. Eyman, *J. Electrochem. Soc.*, **141**, 1698 (1994).
8. F. W. Preston, *J. Soc. Glass Technol.*, **11**, 214 (1927).
9. L. M. Cook, *J. Non-Cryst. Solids*, **120**, 152 (1990).
10. C. W. Liu, B. T. Dai, W. T. Tseng, and C. F. Yeh, *J. Electrochem. Soc.*, **143**, 716 (1996).
11. W. T. Tseng and Y. L. Wang, *J. Electrochem. Soc.*, **144**, L15 (1997).
12. D. Wang, J. Lee, K. Holland, T. Bibby, S. Beaudioin, and T. Cale, *J. Electrochem. Soc.*, **144**, 1121 (1997).
13. O. G. Chekina, L. M. Keer, and H. Liang, *J. Electrochem. Soc.*, **145**, 2210 (1998).
14. D. A. Rigney, *Wear*, **175**, 63 (1965).
15. G. H. Martin, *Kinematics and Dynamics of Machines*, p. 8, McGraw-Hill, Inc., New York (1982).
16. J. Denavit and R. S. Hartenberg, *ASME J. Appl. Mech.*, **77**, 215 (1955).
17. M. W. Walker and D. E. Orin, *ASME J. Dynam. Syst., Meas. Control*, **104** (3), 205 (1982).
18. B. O. Peirce and R. M. Foster, *A Short Table of Integrals*, Ginn & Co., New York (1961).
19. C. Liu, Ph.D. Thesis, National Chiao Tung University, Hsinchu, Taiwan (1996).